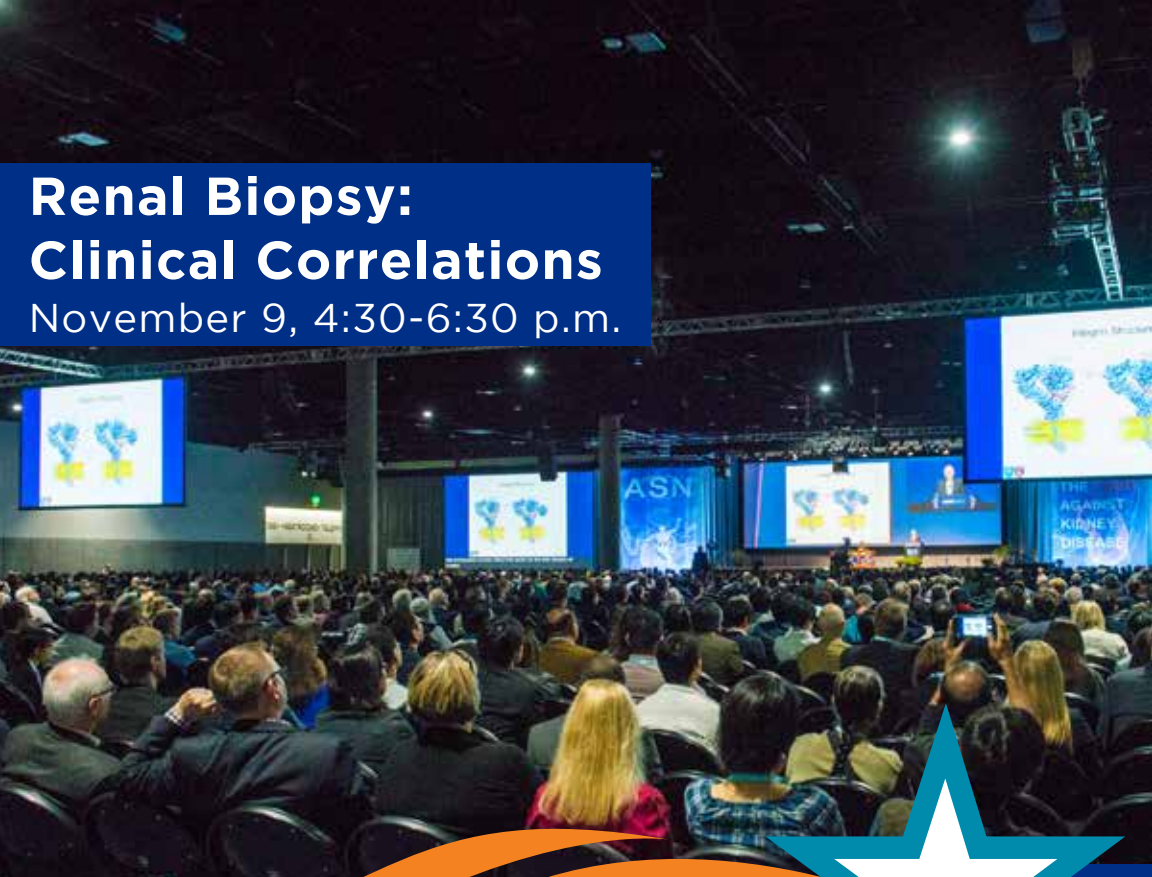

Renal Biopsy: Clinical Correlations

November 9, 4:30-6:30 p.m.

KIDNEY WEEK 2019

Washington, DC | Nov. 5–10

Case 1 from Kammi J. Henriksen, MD – University of Chicago

A 50-year-old man with HIV infection (currently with an undetectable viral load), human herpesvirus 8 (HHV-8) infection, Kaposi sarcoma, and multicentric Castleman disease presented with 2 weeks of fatigue, vomiting, and anorexia. He had recently completed a course of trimethoprim and sulfamethoxazole for cellulitis. Notably, he was diagnosed with HIV infection 13 years prior to admission. He was started on highly active antiretroviral therapy (HAART) with a tenofovir-containing regimen 10 years after the diagnosis of HIV. Despite treatment, his CD4 levels remained low (100-200/μL). His HIV infection was complicated by multicentric Castleman disease, which was diagnosed 1 year prior to admission when the patient presented with fever and bilateral axillary adenopathy. Lymph node biopsy at that time showed follicular hyperplasia with HHV-8–positive cells.

On admission, physical examination was significant for dry mucous membranes, sinus tachycardia, and a diffuse papular rash over his torso and extremities consistent with Kaposi sarcoma. Workup was significant for severe hyponatremia, AKI, and microscopic hematuria with dysmorphic red blood cells (RBCs). Laboratory findings were as follows:

Serum	
Sodium	103 mEq/L
Creatinine	3.7 mg/dL (previous baseline 0.9 mg/dL)
HHV-8	33,700 copies/mL
IL-6	83.2 pg/mL
ANCA	Negative
Antinuclear antibodies	Negative
C3/C4	Negative
Urine	
24-Hour protein	2.1 g
Urine sediment microscopy with renal tubular epithelial cells, granular casts, and RBCs.	

A renal biopsy was performed; representative figures are shown below.

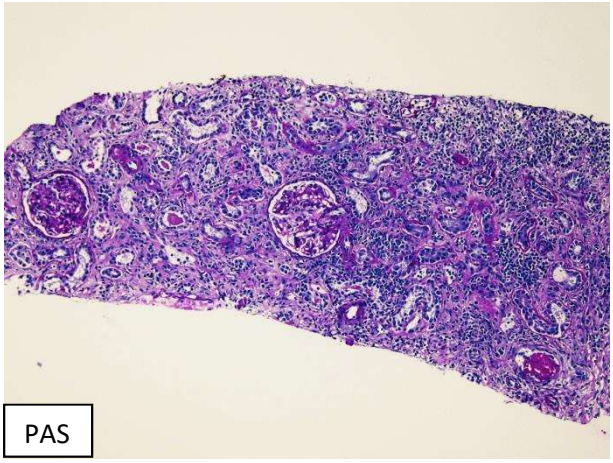
PAS

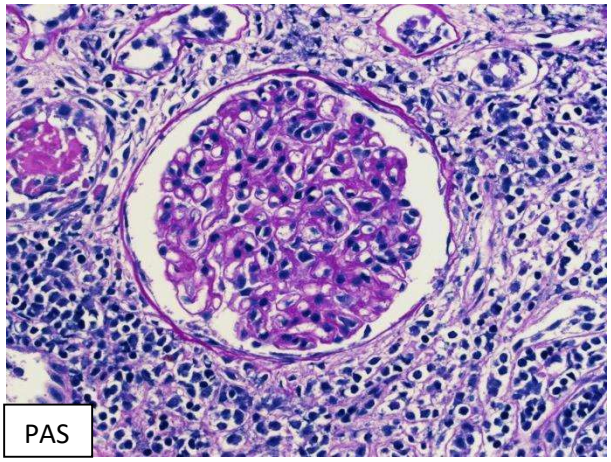
PAS

Periodic acid–Schiff (PAS) stain

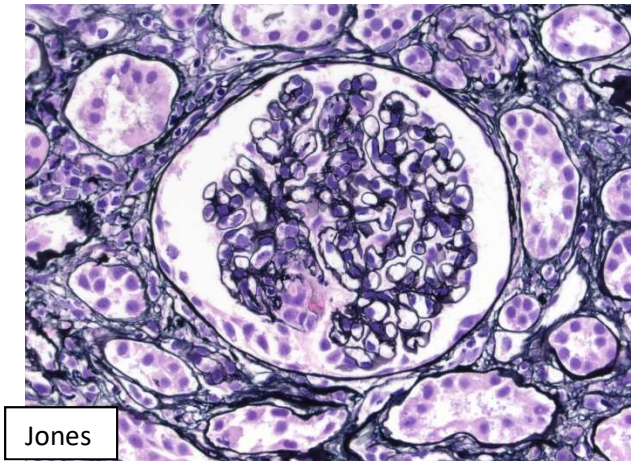

PAS stain

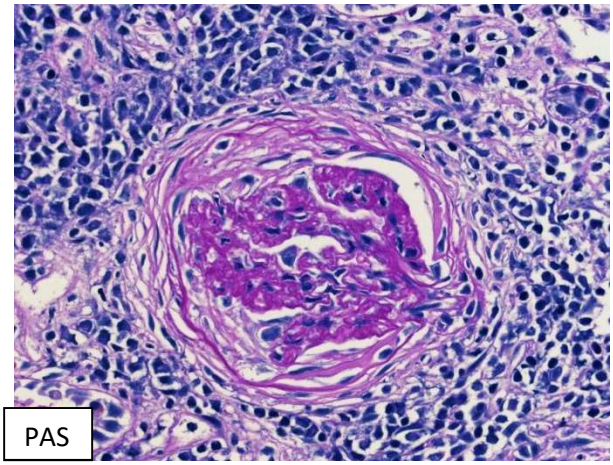

Jones silver stain

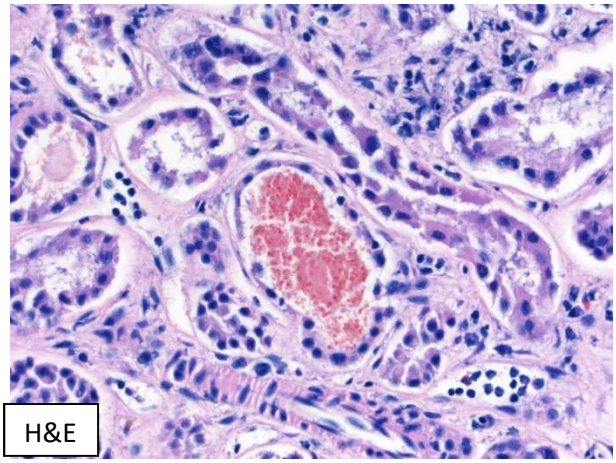

PAS stain

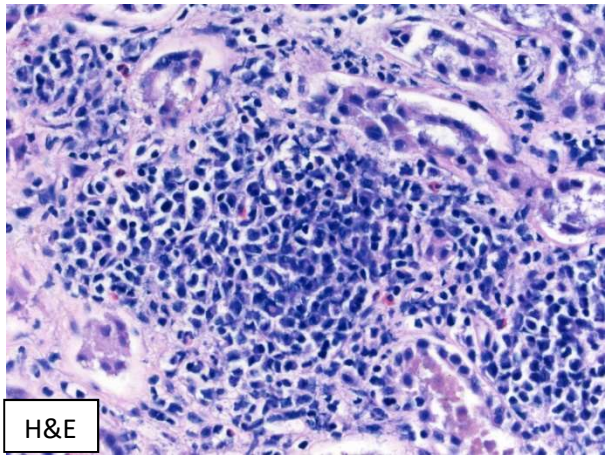

Hematoxylin and eosin (H&E) stain

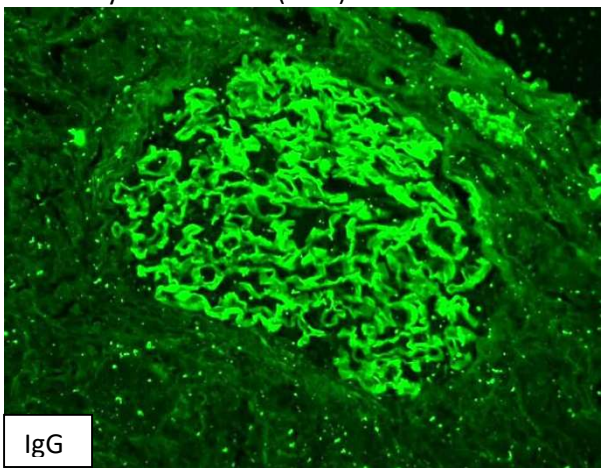

H&E stain

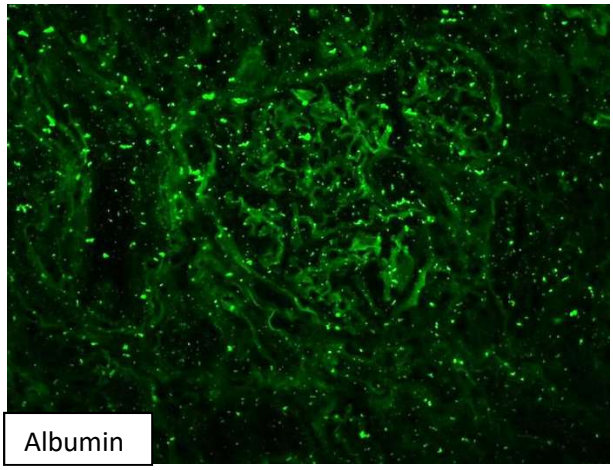

IgG Albumin

Pathologic Findings

Kidney biopsy demonstrated focal necrotizing and crescentic GN, with 1 glomerulus (of 18) showing segmental fibrinoid necrosis with associated rupture of the GBMs, 1 glomerulus showing a possible fibrous crescent and periglomerular inflammation, and 2 glomeruli with global sclerosis. The remaining glomeruli showed occasional circulating inflammatory cells but were otherwise unremarkable. There was diffuse lymphoplasmacytic interstitial inflammation and tubulitis, and there were occasional intratubular RBC casts. By direct immunofluorescence (on a scale of 0–4+), there was diffuse linear staining of the GBMs for IgG (3+) and κ and λ light chains (2–3+ each). Ultrastructural evaluation showed occasional endothelial cell swelling and extensive podocyte foot process effacement. There were no immune-type electron dense deposits. Overall, the findings were consistent with anti-GBM nephritis and diffuse lymphoplasmacytic interstitial nephritis.

Clinical Follow-up

An anti-GBM titer was sent and returned positive at 4.2 antibody index (reference range 0.0–0.9). Treatment was initiated with steroids, cyclophosphamide, and plasmapheresis, but the patient's renal function continued to deteriorate. He subsequently developed gross hematuria, worsening anemia, new thrombocytopenia, and uremic symptoms requiring dialysis. Three weeks after diagnosis, he started an intensive course of rituximab, which led to rapid clinical improvement and renal recovery. Nine weeks after diagnosis, dialysis was discontinued. At that time, anti-GBM and HHV-8 levels were undetectable, and IL-6 levels improved to 8.5 pg/mL. At a 6-month follow-up, his serum creatinine was 2.2 mg/dL with <1 g/d proteinuria and further improvement in IL-6 levels to 3.11 pg/mL.

Questions for Case 1:

1. What is the morphologic pattern of glomerular injury?
    A. Exudative GN
    B. Mesangial proliferative GN
    C. Membranoproliferative GN
    D. Necrotizing and/or crescentic GN
    E. Collapsing glomerulopathy

Light microscopy demonstrates a focal necrotizing GN with associated rupture of the GBMs, best visualized on Jones silver staining. One glomerulus also demonstrates a possible fibrous crescent and periglomerular inflammation. The remaining glomeruli are unremarkable aside from occasional circulating inflammatory cells. There is no mesangial or endocapillary hypercellularity, no duplication of the GBMs, and no evidence of collapsing glomerulopathy.

2. Based on the immunofluorescence findings, what disease is favored in the differential diagnosis?
    A. Pauci-immune GN
    B. Postinfectious GN
    C. Collapsing glomerulopathy

D. Anti-GBM nephritis
E. HIV-associated immune complex GN with lupus-like features

Immunofluorescence microscopy demonstrates diffuse linear staining of the GBMs for IgG, consistent with anti-GBM nephritis. No or minimal immunofluorescence staining would be expected in pauci-immune GN and collapsing glomerulopathy. Granular immune complex deposits would be seen in postinfectious GN and HIV-associated immune complex GN.

3. What are potential underlying causes of the tubulointerstitial inflammation?
   A. Drug hypersensitivity or toxicity
   B. HIV infection
   C. Castleman disease
   D. GM
   E. All of the above

Light microscopy demonstrates diffuse tubulointerstitial inflammation composed predominantly of lymphocytes and plasma cells, with rare scattered eosinophils. Tubulointerstitial nephritis in this patient may be due to a number of underlying factors. Drug-associated acute interstitial nephritis can be seen in association with antibiotic use and HAART. HIV infection (HIV associated nephropathy) is often accompanied by interstitial nephritis that may be predominantly plasmacytic in nature. Renal involvement by Castleman disease can manifest as interstitial nephritis. Furthermore, GN often causes secondary interstitial inflammation.

4. What is the most common pattern of renal injury in patients with Castleman disease?
   A. Thrombotic microangiopathy-like lesions
   B. AA amyloidosis
   C. Interstitial nephritis
   D. Anti-GBM nephritis
   E. FSGS

Two large studies have demonstrated that thrombotic microangiopathy-like lesions are the most frequent renal involvement in Castleman disease. These lesions include endothelial swelling, glomerular double contours, glomerular and arteriolar thrombi, and mesangiolysis. Other patterns of renal injury have been reported in Castleman disease, including AA amyloidosis, interstitial nephritis, anti-GBM nephritis, and FSGS, but these are less common than the vascular lesions.

Diagnosis

Anti-GBM nephritis and diffuse lymphoplasmacytic interstitial nephritis.

Discussion

A wide spectrum of renal manifestations can be seen in patients who are HIV positive.[1-2] Common glomerular diseases include podocytopathies (e.g., minimal change disease, FSGS with or without collapsing features) and immune complex–mediated glomerulopathies (e.g., IgA

nephropathy, membranous nephropathy, lupus-like nephritis). There have also been rare reports of HIV infection and concomitant anti-GBM nephritis,[3-6] underscoring the need for renal biopsy in patients who have HIV infection. Clinical assessment and diagnosis is complicated by the fact that HIV-positive patients can produce a variety of autoantibodies due to humoral dysregulation and polyclonal B-cell activation. Notably, anti-GBM antibodies are present in 17% of HIV-infected patients,[7] but the presence of these antibodies is not associated with clinical manifestations of anti-GBM disease in most cases.[8-9] Thus, even with a positive serologic test, kidney biopsy may be necessary to demonstrate the presence or absence of renal involvement.

Anti-GBM disease is a rare small-vessel vasculitis that can affect the glomerular capillaries, the pulmonary capillaries, or both (termed Goodpasture syndrome).[10] The pathogenic role of anti-GBM antibodies has been well documented. The principal antigenic target is the noncollagenous (NC1) domain of the α3 chain of type IV collagen (the "Goodpasture antigen"), which is expressed in the basement membranes of the glomerular and alveolar capillaries. It is possible that HIV infection of the glomerular capillaries or podocytes causes endothelial or podocyte injury that damages the underlying GBM and unmasks the antigen. Most patients with anti-GBM disease present with features of rapidly progressive GN, including AKI, hypertension, and hematuria, with concurrent pulmonary hemorrhage in 30%–60% of patients. Increasingly recognized "atypical" presentations are characterized by a more indolent clinical course, absence of lung involvement, and undetectable circulating anti-GBM antibodies.[11]

In classic anti-GBM nephritis, kidney biopsy demonstrates a diffuse necrotizing and crescentic GN, often involving >75% of the glomeruli. The crescents are predominantly acute (cellular) crescents of uniform age. There is frequent rupture of the GBMs with associated fibrinoid necrosis. Atypical or mild forms may show minimal glomerular lesions with few crescents, mesangial or endocapillary proliferation, membranoproliferative features, or lobular mesangial expansion. Direct immunofluorescence demonstrates the hallmark bright linear IgG staining of the GBMs with a high sensitivity (99%), which is the gold standard for diagnosis of anti-GBM disease. There is usually linear staining for C3 and κ and λ light chains. Electron microscopy demonstrates nonspecific features, including GBM rupture or fibrinoid necrosis. Electron microscopy is primarily useful to exclude concomitant glomerular pathologies or other diseases that may have linear GBM immunofluorescence staining (e.g., fibrillary GN, monoclonal immunoglobulin deposition disease). Standard treatment for anti-GBM disease includes plasmapheresis to remove the pathogenic autoantibodies, along with cytotoxic therapy (cyclophosphamide) and immunosuppression (high-dose corticosteroids).

Castleman disease (or angiofollicular lymph node hyperplasia) is a rare lymphoproliferative disorder found with a higher frequency in patients who are HIV positive. The incidence of HIV-associated multicentric Castleman disease appears to be increasing in the HAART era. Multicentric Castleman disease is characterized by multiple regions of lymphadenopathy and systemic inflammatory symptoms such as hepatosplenomegaly, cytopenias, and organ dysfunction due to excessive pro-inflammatory hypercytokinemia. HHV-8 and cytokine dysregulation, including increased levels of vascular endothelial growth factor and IL-6, are thought to play a role in the pathogenesis of HIV-associated multicentric Castleman disease. Rituximab is often used alone or in combination with chemotherapy for treatment of multicentric Castleman disease. Several studies have demonstrated renal involvement in 25%–54% of Castleman disease cases.[12-13] The most common renal manifestations are thrombotic microangiopathy–like lesions (e.g., endothelial swelling, glomerular double contours, glomerular/arteriolar thrombi, mesangiolysis). Other patterns of renal injury include AA amyloidosis, interstitial nephritis, and FSGS. Underlying multicentric Castleman disease may have contributed to the lymphoplasmacytic interstitial nephritis in our case.

Temporally, the diagnosis of HHV-8–associated multicentric Castleman disease in our case was made 1 year prior to the onset of anti-GBM disease, raising the possibility that the two entities might be linked. Specifically, we wondered whether the Castleman disease–associated tumor cells may be the source of the anti-GBM antibodies. Interestingly, there is a recent report of three patients with both anti-GBM disease and Castleman disease with a similar clinical and temporal onset of the two diseases.[14] The authors tested a similar hypothesis in one patient with lymph node biopsy specimens available and found sporadic plasma cells producing α3(IV)NC1-IgG, suggesting a causal relationship between Castleman disease and the development of anti-GBM disease.

References

1. Swanepoel CR, Atta MG, D'Agati VD, et al. Kidney disease in the setting of HIV infection: conclusions from a Kidney Disease: Improving Global Outcomes (KDIGO) Controversies Conference. *Kidney Int*. 2018;93:545–559.

2. Zaidan M, Lescure FX, Brocheriou I, et al. Tubulointerstitial nephropathies in HIV-infected patients over the past 15 years: a clinico-pathological study. *Clin J Am Soc Nephrol*. 2013;8:930–938.

3. Hartle PM, Carlo ME, Dwyer JP, Fogo AB. AKI in an HIV patient. *J Am Soc Nephrol*. 2013;24:1204–1208.

4. Monteiro EJB, Caron D, Balda CA, Franco M, Pereira AB, Kirsztajn GM. Anti-glomerular basement membrane glomerulonephritis in an HIV positive patient: case report. *Braz J Infect Dis*. 2006;10:55–58.

5. Wechsler E, Yang T, Jordan SC, Vo A, Nast CC. Anti-glomerular basement membrane disease in an HIV-infected patient. *Nat Clin Pract Nephrol*. 2008;4:167–171.

6. Singh P, Barry M, Tzamaloukas A. Goodpasture's disease complicating human immunodeficiency virus infection. *Clin Nephrol*. 2011;76:74–77.

7. Hernandez GT, Critchfield JM, Rodriguez RA. Interpretation of serologic tests in an HIV-infected patient with kidney disease. *Nat Clin Pract Nephrol*. 2006;2:708–712.

8. Szczech LA, Anderson A, Ramers C, et al. The uncertain significance of anti-glomerular basement membranes antibody among HIV-infected persons with kidney disease. *Am J Kidney Dis*. 2006;48:e55–e59.

9. Minocha V, Makary R, Poenariu A. An unusual case of anti-GBM antibody elevation in HIV-associated nephropathy. *Case Rep Nephrol*. 2014;2014;956475.

10. McAdoo SP, Pusey CD. Anti-glomerular basement membrane disease. *Clin J Am Soc Nephrol*. 2017;12(7):1162–1172.

11. Nasr SH, Collins AB, Alexander MP, et al. The clinicopathologic characteristics and outcome of atypical anti-glomerular basement membrane nephritis. *Kidney Int*. 2016;89(4):897–908.

12. Xu D, Lv J, Dong Y, et al. Renal involvement in a large cohort of Chinese patients with Castleman disease. *Nephrol Dial Transplant*. 2012;27:iii119–iii125.

13. El Karoui K, Vuiblet V, Dion D, et al. Renal involvement in Castleman disease. *Nephrol Dial Transplant*. 2011;26:599–609.

14. Gu Q, Jia X, Hu S, et al. The clinical and immunologic features of patients with combined anti-GBM disease and Castleman disease. *Am J Kidney Dis*. 2018;71:904–908.

Case 2 from François Gougeon, MD, FRCPC -- Centre hospitalier de l'université de Montréal (CHUM)

A 69-year-old white man presented with slowly progressive chronic renal failure over a 6-year period. He had a history of obesity, dyslipidemia, hepatic steatosis, benign prostatic hyperplasia, and mild hypertension. Through his work as a hairdresser, he had been exposed to hair dye. A proximal tubulopathy without acidosis was also present.

The patient was asymptomatic. His serum creatinine concentration was elevated to 1.5 mg/dL (GFR mL/min/1.73 m^2) from a baseline of 0.7–0.8 mg/dL (GFR >60 mL/min/1.73 m^2). Proximal tubulopathy was characterized by hypophosphatemia (0.55 mmol/L), elevated urine phosphate (39.7 mmol/L), elevated urinary amino acids, and glycosuria despite normal glycemia. Hypophosphatemia persisted despite vitamin D repletion.

Prior to renal biopsy, the patient had subnephrotic-range proteinuria of up to 1.6 g/24 hours, with normal serum albumin. His results had one positive serology for antinuclear antibodies (ANA) (titer = 1/160) 2 years before renal biopsy with negative controls afterwards (prior to treatment). No symptoms of systemic lupus erythematosus (SLE) or other connective tissue diseases were ever observed or reported by the patient.

Serologies were otherwise negative for anti-DNA, anti-Jo, Scl-70, perinuclear ANCA, cytoplasmic ANCA, hepatitis B, hepatitis C, HIV, SSA, and SSB. Serum complement factors C3 and C4 were within normal range. Serum protein electrophoresis was within normal limits, with a normal κ/λ light chain ratio.

A kidney biopsy was performed in 2018.

Pathologic Findings

Light microscopy examination was done on fragments of renal cortex containing up to 18 glomeruli, of which 2 were globally sclerotic. Nonsclerotic glomeruli showed no significant histological alterations. The tubulointerstitial compartment showed mild fibrosis and tubular atrophy involving approximately 15% of the sampled tissue. The main histological finding consisted of acute tubular injury, characterized by simplification of tubular epithelial cells, focal loss of brush border, vacuolization of tubular cell cytoplasm, and reactive nuclear changes. Arteries showed only mild arteriosclerosis, without evidence of acute vasculopathy or vasculitis.

There was very little interstitial inflammation noted. Most of the interstitial inflammation consisted of mononucleated leukocytes in proximity to sclerotic glomeruli or larger vessels. No tubulitis was noted. The histological features were thus not characteristic of acute interstitial nephritis.

Direct immunofluorescence showed strong (3+) granular staining along tubular basement membranes and Bowman's capsule for IgG, C3, κ, and λ. IgG subclasses showed staining in the same pattern and intensity for IgG1 and IgG4. There was only trace staining in the glomerular tuft.

Electron microscopy showed abundant electron-dense deposits along tubular basement membranes. These deposits did not show any substructure. There were no electron-

dense deposits identified along GBMs or in the mesangial areas. No tubuloreticular inclusions were identified.

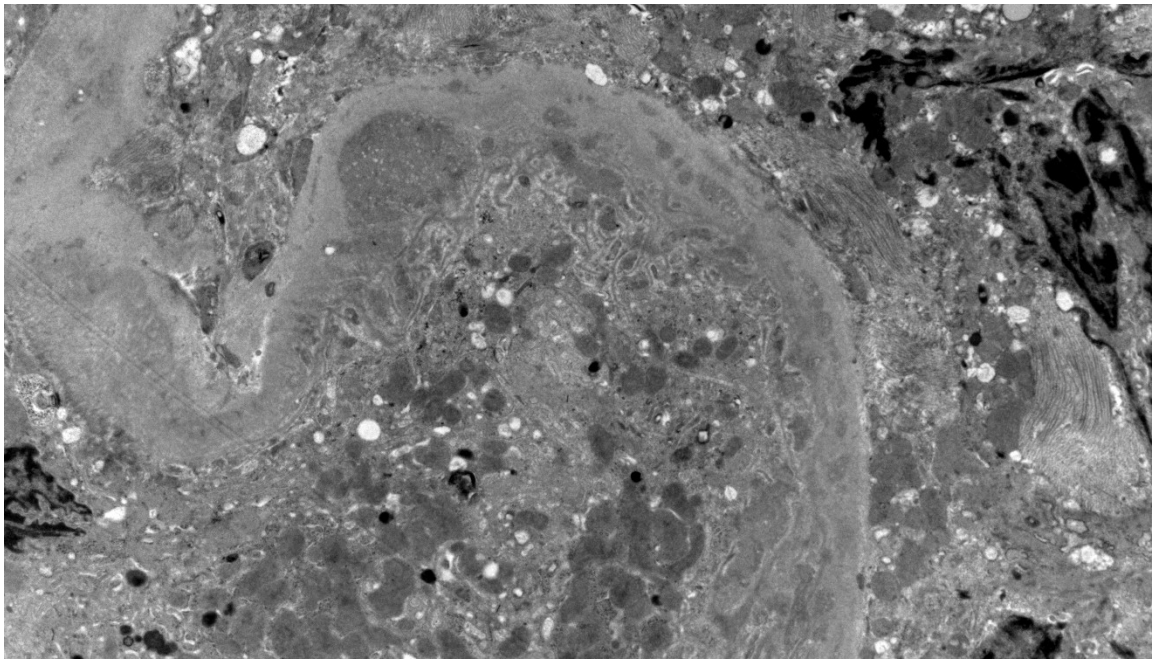

The patient's serum was sent for indirect immunofluorescence for the detection of anti-brush border antibodies (ABBA), and the result was positive (presence of ABBA IgG in the patient's serum reactive to the proximal tubular brush border on a section of normal kidney). Tissue was also tested for low density lipoprotein–related protein 2 (LRP2), also known as megalin; the result was negative.

Clinical Follow-up

The patient was treated with corticosteroids with subsequent normalization of serum creatinine. Unfortunately, the treatment had to be discontinued after 3 months because of a severe adverse reaction. Proximal tubulopathy symptoms have persisted despite normal renal function, and the patient is currently being evaluated for other immune-suppressive treatments.

Questions for Case 2:

1. What is the main histological finding in Figure 1?

A. Acute interstitial nephritis
B. Mesangial proliferative glomerulonephritis
C. Acute tubular injury
D. Storiform fibrosis
E. No significant histological changes are present

Figure 1:

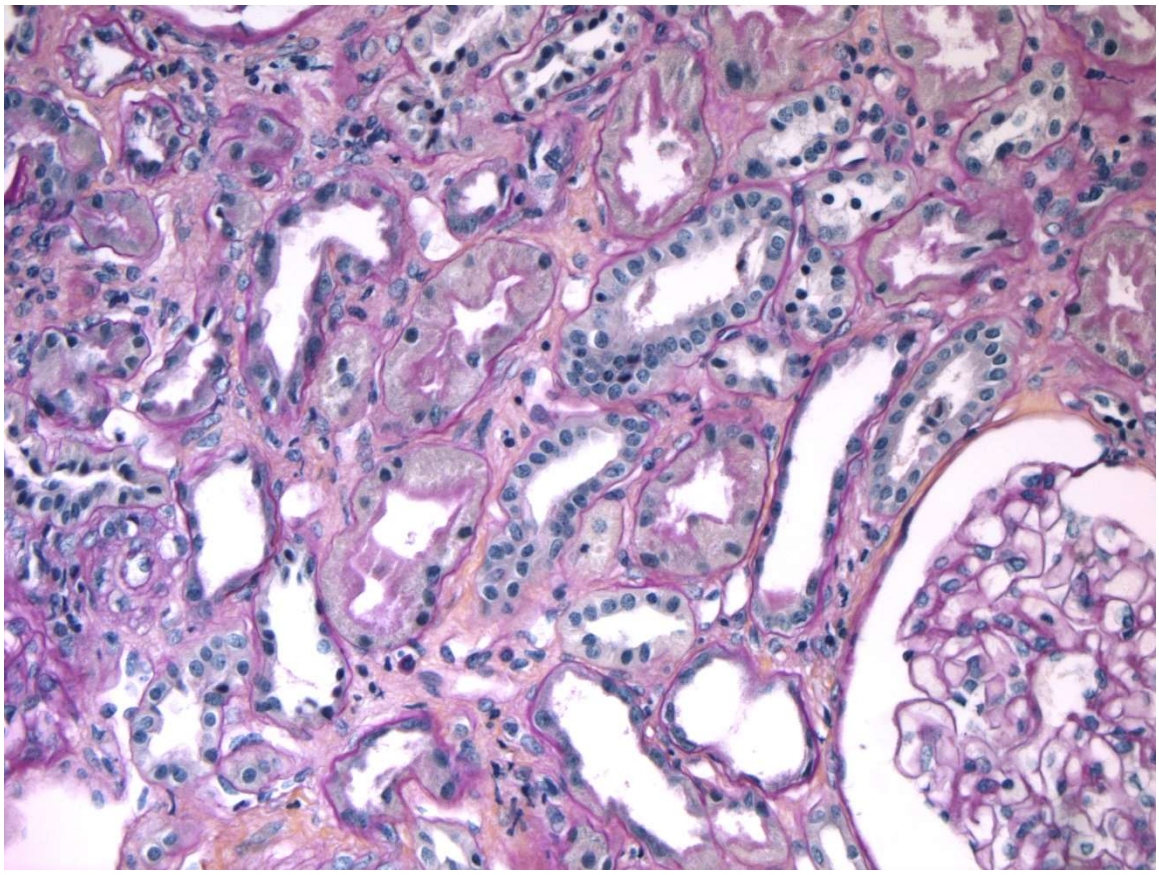

This micrograph shows tubules with signs of acute tubular injury. The most striking feature is the "simplification" or flattening of epithelial cells. The lush, reddish appearance of the brush border is lost in areas. Rare lymphocytes are scattered throughout the interstitium, without any tubulitis. This figure is not diagnostic of acute interstitial nephritis. Only minimal fibrosis is present. The part of the glomeruli seen here is unremarkable.

2. How would you characterize the staining pattern for IgG seen in Figure 2?

A. Linear tubular basement membrane staining
B. Diffuse strong granular staining along the tubular basement membrane and GBM
C. Granular staining along the tubular basement membranes only
D. Granular staining along the tubular basement membrane and Bowman's capsule
E. Nonspecific background staining

Figure 2:

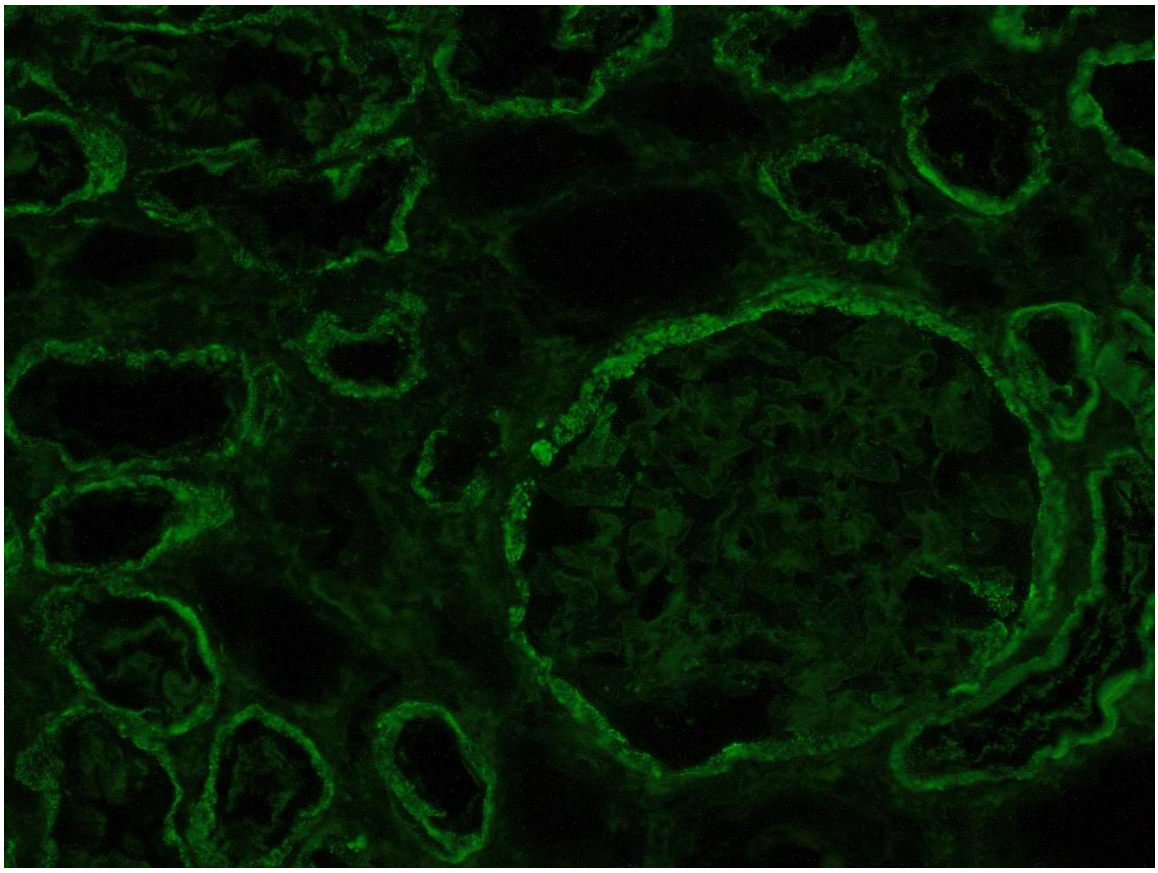

This figure from direct immunofluorescence for IgG shows strong granular deposits along the proximal tubule basement membrane and Bowman's capsule. The glomerular tuft shows only trace nonspecific staining.

3. Which of these entities does NOT present with tubular basement membrane immunoglobulin deposits?

A. Paraphenylenediamine hair dye nephropathy
B. IgG4 disease–associated nephropathy
C. Sjögren disease
D. Lupus nephritis
E. ABBA-associated nephropathy

Paraphenylenediamine hair dye nephropathy has been associated with rhabdomyolysis and other toxic changes but not with the deposition of immune complexes. Lupus nephritis, Sjögren disease, and IgG4 disease can all be associated with tubular basement membrane deposits. Those entities are also usually associated with systemic symptoms and positive serologies in SLE and Sjögren. ABBA disease is kidney-restricted and presents with tubular basement membrane and Bowman's capsule immune complex deposits.

Diagnosis

ABBA disease.

Discussion

This case showed a nonspecific pattern on light microscopy, with only tubular injury and mild interstitial fibrosis. The key finding for this case was the deposition of immune complex deposits along the tubular basement membranes and Bowman's capsule as seen on direct immunofluorescence and confirmed by electron microscopy. This pattern is characteristic of ABBA disease and prompted serological testing for this entity, which was positive.

ABBA disease (also referred to as anti-brush border tubulointerstitial nephritis) is an extremely rare disease, perhaps underrecognized, that is caused by circulating antibodies to proximal tubule brush border antigens. It was first described as "primary tubulointerstitial nephritis caused by antibodies to proximal tubular antigens"[3]. It predominantly affects men in the sixth to eighth decade of life. Most reported cases present with AKI and subnephrotic proteinuria, although cases of slowly progressive renal failure have also been described. At least one case of recurrence in a transplanted kidney has been reported.[1]

Until recently, cases of ABBA disease were associated in the literature with acute interstitial nephritis on light microscopy. However, a recent report of 10 cases of ABBA disease showed a range of morphological changes, with most cases (6/10) presenting only acute tubular injury with little to no interstitial inflammation.[2] All cases showed IgG and C3 staining along the tubular basement membrane and Bowman's capsule. Most cases also showed weaker segmental staining along GBMs, although this was not observed in our case.

The differential diagnosis of ABBA disease includes other entities that can present with granular tubular basement membrane deposits. These include Sjögren disease, SLE, and IgG4 disease. Sjögren disease usually presents with acute tubulointerstitial nephritis rich in plasma cells and features other systemic symptoms and positive serologies (SSA, SSB, ANA). Lupus nephritis usually presents with a "full-house" staining pattern, glomerular disease, systemic symptoms, and positive ANA results. Although ANA results were positive at one time in this patient, all controls were negative, even before treatment, and no other features of SLE were present. IgG4 disease should show restriction with IgG4 subclass on immunofluorescence and a plasma-cell rich infiltrate with storiform fibrosis on light microscopy. None of these entities have been reported to be associated with positive anti-brush border staining on indirect immunofluorescence with patient serum on normal kidney tissue.

LRP2 or megalin has recently been identified as the antigen responsible for this disease in a series of 10 cases of ABBA disease.[2] Although our case did not show staining for LRP2/megalin, this could be due to a technical issue because native kidney biopsies at our institution are fixed in Duboscq-Brasil solution instead of formalin. It is also possible that another antigen is responsible for the disease in this case.

Although light microscopy showed only acute tubular injury, direct immunofluorescence staining revealed the deposition of polyclonal granular IgG deposits along the tubular basement membranes and Bowman's capsule. This prompted indirect immunofluorescence testing with the patient's serum, which confirmed the presence of antibodies reacting to the brush border of normal kidney, confirming the diagnosis of ABBA disease. ABBA disease is an extremely rare condition affecting elderly patients and presenting with acute or slowly progressive renal failure.

References

2. Larsen CP, Trivin-Avillach C, Coles P, et al. LDL receptor-related protein 2 (megalin) as a target antigen in human kidney anti-brush border antibody disease. *J Am Soc Nephrol*. 2018;29(2):644–653.

1. Rosales IA, Collins AB, do Carmo PA, Tolkoff-Rubin N, Smith RN, Colvin RB. Immune complex tubulointerstitial nephritis due to autoantibodies to the proximal tubule brush border. *J Am Soc Nephrol*. 2016;27(2):380–384.

3. Morrison EB, Kozlowski EJ, McPhaul JJ Jr. Primary tubulointerstitial nephritis caused by antibodies to proximal tubular antigens. *Am J Clin Pathol*. 1981;75(4):602–609.

Case 3 from Kelly D. Smith, MD PhD -- The University of Washington

A 27-year-old African American man with no significant medical history presented in January 2005 with a fever, headache, nausea, vomiting, and abdominal discomfort and subsequently developed acute renal failure with a creatinine of 2.3 mg/dL. He also presented with a nephrotic range of proteinuria (4 g/24 hours). A renal biopsy was performed at that time and showed FSGS (classified as the cellular variant) and acute tubular injury (Figure 1).

The patient was treated with hydration and antibiotics for chronic sinusitis. Workup for the etiology of the acute renal failure, including infectious agents and rheumatologic diseases, was negative. The patient recovered and became afebrile. He was discharged home on February 18, 2005, from a local hospital. At the time of discharge, his creatinine value had returned to 1.1 mg/dL, but nephrotic syndrome persisted.

The patient felt well and returned to work without any trouble until May 11, 2005, when his fever started again (temperature up to 104°F), which was accompanied by nausea, vomiting, diarrhea, and abdominal discomfort but no headache. He was found to have severe renal failure (serum creatinine 14.2 mg/dL), anuria, and nephrotic range proteinuria and was transferred to the University of Washington Medical Center for further workup and management. Notable laboratory test results included monocytosis and mild thrombocytopenia but no leukocytosis, elevated lactate dehydrogenase and erythrocyte sedimentation rate, and markedly elevated ferritin. The constellation of the patient's symptoms did not fit common rheumatic diseases such as lupus or vasculitis. With the markedly elevated ferritin, adult onset of Still disease was considered; however, the patient did not meet criteria for Still disease.

A second kidney biopsy was performed.

Questions for Case 1:

1. What is the least likely etiology for the pathogenic finding below?
    A. HIV infection
    B. Pamidronate
    C. Diabetes
    D. Parvovirus infection
    E. None of the above

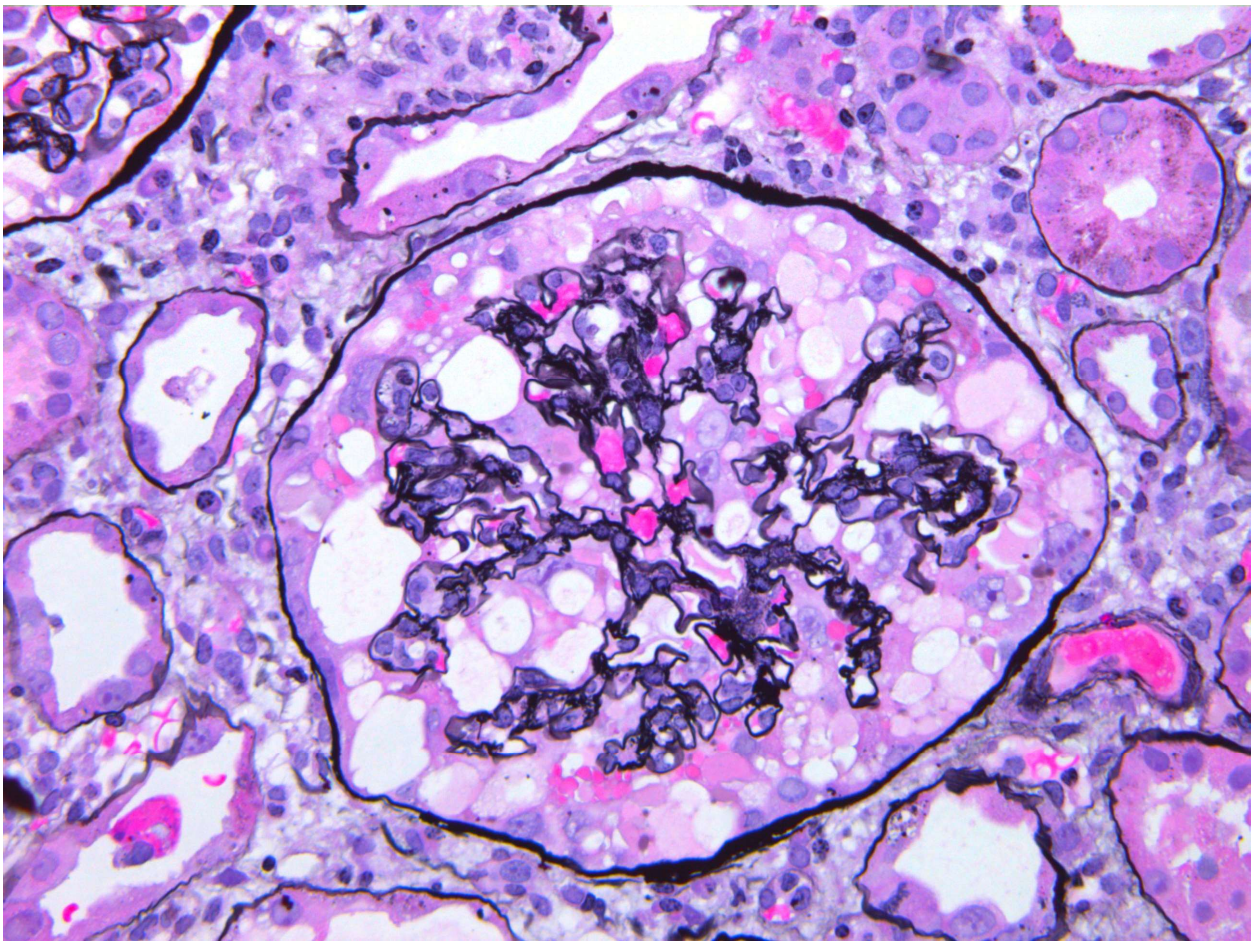

Numerous factors have been associated with the development of collapsing glomerulopathy. These include drugs such as pamidronate and interferons, viral infections (HIV, parvovirus, cytomegalovirus, hepatitis C), severe vascular disease, and autoimmune diseases. Although collapsing glomerulopathy has been described in diabetes, this lesion is superimposed on the nodular glomerulosclerosis seen in diabetic nephropathy. The glomerulus in this figure has no obvious underlying pathology and definitely no features of diabetic glomerular injury.

2. What are the histologic features in the figure above that define collapsing glomerulopathy?
    A. Segmental or global collapse of the capillary loops and podocyte hypertrophy
    B. Intracapillary foam cells occluding lumina
    C. Hyaline occlusion of capillary loops adjacent to the vascular pole
    D. Occlusion of capillary loops by cells or hyaline and attachment to Bowman's capsule adjacent to the tubuloglomerular junction

The photomicrograph shows a glomerulus with near global collapse of the capillary loops. There are only rare leukocytes in the capillary loops and no significant

endocapillary hypercellularity. The urinary space is filled with cells that contain prominent cytoplasmic vacuoles that range from clear to eosinophilic. The cells in the urinary space are not contiguous with the parietal epithelium, and there are no obvious leukocytes in the urinary space. These changes in the urinary space represent podocyte hypertrophy and hyperplasia. Together, the above findings establish the histologic diagnosis of collapsing glomerulopathy. Pertinent negative findings that eliminate other possibilities include the lack of features seen in a cellular crescent, described above, and the lack of hyaline accumulation or segmental obliteration of capillary loops adjacent to the tubuloglomerular junction or vascular pole.

3. Which of the following histologic findings are associated with *APOL1* risk allele dizygosity?
    A. Collapsing glomerulopathy
    B. Tubular microcystic change
    C. Tip variant of FSGS
    D. A and B
    E. B and C
    F. All of the above

All of the above histologic changes are associated with kidney diseases seen in patients with two risk alleles of* APOL1*. Collapsing glomerulopathy and tubular microcystic change are classic features of HIV-associated nephropathy, which has one of the strongest associations with* APOL1*. Tubular microcystic change, along with thyroidization-type tubular atrophy and solidified-type glomerulosclerosis are also associated with* APOL1 *risk allele genotype in CKD.

4. Which of the following would be the LEAST helpful in determining the best immediate treatment plan for his disease?
    A. Test for HIV infection and other viral infections
    B. Genotype *APOL1* genes
    C. Look for autoimmune disease
    D. Look for malignancies
    E. Look for potential drugs

It is critical to determine whether this patient has a disorder or exposure that is associated with collapsing glomerulopathy and in particular this very aggressive form that has prominent tubulointerstitial injury and inflammation. Identifying a potential causative agent will help determine what to therapeutically target in this patient, because treating this process is the best approach to addressing the patient's kidney disease. In this patient, the pathologic findings are highly suggestive of an interferon-induced injury, and a search for potential sources of interferon (infections, drugs, autoimmune diseases, and malignancies) should be the first consideration. Although* APOL1 *genotyping may help better define the pathogenesis of this patient's disease and his family's potential risk for kidney disease, this information will not lead to an immediate action.

<u>Diagnosis</u>

FSGS, collapsing variant, with acute tubular injury, tubular microcystic change, and associated interstitial inflammation, consistent with *APOL1*-associated collapsing glomerulopathy.

Review of Case 3 Pathology and Differential Diagnosis

The whole-slide images demonstrate sections of renal cortex containing about 14–17 glomeruli, of which 7–10 glomeruli exhibit segmental lesions. Segmental changes in these glomeruli are characterized by varying degrees of shrinkage and collapse of the capillary loops with associated hypertrophy and hyperplasia of overlying visceral epithelial cells, which also contain prominent clear and eosinophilic cytoplasmic vacuoles. The segmental lesions of 1–3 glomeruli show solidification of capillary tufts and increased matrix deposition. In some glomeruli, there is segmental, mild increase in endocapillary cellularity.

FSGS has been subdivided into five histologic variants: not otherwise specified (NOS), perihilar, cellular, tip, and collapsing.[1] The presence of segmental and global collapse of glomerular capillary loops with hypertrophy and hyperplasia of the overlying podocyte seen in this case meet the diagnostic criteria for the collapsing variant of FSGS.[1]

The biopsy also demonstrates extensive tubular injury characterized by diffuse attenuation of the proximal tubular epithelial cells, loss of brush borders, vacuolization of epithelial cytoplasm, and sloughing of degenerating tubular epithelial cells into luminal spaces. Many tubules are markedly dilated with attenuated epithelium, forming microcysts that are filled with proteinaceous material. There are also numerous hyaline and granular casts within the tubular luminal spaces. The peritubular interstitium is diffusely edematous and infiltrated by mononuclear leukocytes, including frequent plasma cells. Some tubules are infiltrated by inflammatory cells. These findings establish concurrent tubular injury and tubulointerestitial nephritis, with tubular microcystic change.

The lack of significant global glomerulosclerosis, interstitial fibrosis, and tubular atrophy is consistent with the clinical history of this patient's disease and a subacute disease process with limited chronicity that has evolved over the past couple of months. The pathologic findings support the diagnosis of collapsing glomerulopathy, and the pathologic changes are suggestive of a genetic background of two *APOL1* risk alleles. The clinical data provided fail to document known factors that cause *APOL1*-associated collapsing glomerulopathy and specifically demonstrate that this patient's disease is not associated with HIV infection. The diagnosis of *APOL1*-associated collapsing glomerulopathy should be suggested in this case, given the pathologic and clinical data, and this should prompt the clinician to investigate for potential etiologies of the collapsing glomerulopathy.

Discussion

The pathologic findings point to a glomerular disorder that has prominent cellularity within the urinary space; the possibility of a crescentic lesion is lessened by the lack of definitive layering of epithelial cells, the lack of inflammatory cells in the urinary space, the integrity of Bowman's capsule, and the lack of glomerular necrosis (disruption of capillary loops with accumulation of fibrin). The findings of capillary collapse with hypertrophy and hyperplasia of the overlying podocytes define this lesion as the collapsing variant of FSGS. This pathologic diagnosis also

correlates well with the patient's clinical history of nephrotic range proteinuria. The biopsy also demonstrate prominent tubular injury, tubular microcystic change, and interstitial inflammation. The combination of collapsing glomerulopathy and these tubulointerstitial changes was first recognized in the setting of HIV infection and what is now commonly termed HIV-associated nephropathy (HIVAN).[2,3]

The pathogenesis of HIV-associated nephropathy was initially postulated to involve direct HIV infection of renal epithelial cells. Although not all labs have been able to reproduce the finding of HIV nucleic acids in renal epithelial cells, transgenic mouse models demonstrated that expression of HIV proteins in podocytes can induce a murine version of FSGS. An alternative hypothesis for direct infection is the production of interferons during infection, which acts on renal epithelial cells in susceptible individuals. This is supported by the findings that multiple viral infections or therapy with interferons (type I and II) can induce disease that mimics HIVAN.[4,5]

The other key ingredient in the pathogenesis of HIVAN is genetic background, because nearly all reported cases of HIVAN affect people of African ancestry.[5] This strong ethnic linkage to the disease has been connected to the *APOL1* gene.[6] (6). The G1 and G2 *APOL1* alleles are protective against *Trypanosoma* infection; however, individuals who carry any combination of these two alleles (risk alleles) have increased risk for several kidney diseases.[7] Patients infected with HIV have a dramatically increased risk for HIVAN—approximately 29-fold in the United States and 80-fold in South Africa.[6] In addition to HIVAN, the *APOL1* genotype also influences several other kidney diseases, including FSGS, lupus nephritis, arterionephrosclerosis, membranous nephropathy, and diabetic nephropathy.[7]

The pathogenic mechanisms that contribute to increased risk for kidney disease in individuals who have two *APOL1* risk alleles is an active area of investigation. As mentioned above, the *APOL1* genotype influences diverse kidney diseases that cover a broad range of etiologies. For a subset of these diseases, there is compelling evidence to support roles for type I and II interferons in the pathogenesis. Innate immune stimuli and in particular type I and II interferons are potent inducers of *APOL1* gene expression in the kidney,[8] suggesting interferon production is a unifying risk factor for some of *APOL1*-associated kidney diseases (i.e., FSGS associated with viral infections and some neoplasms and lupus nephritis).

Testing for infections, autoimmune diseases, and neoplasms was repeated after the kidney biopsy, and the patient was diagnosed with natural killer (NK) cell leukemia. NK cells are notorious for their ability to produce interferon-γ, and for this patient, NK cell leukemia–associated interferon production is a likely cause of his kidney disease. The patient's bone marrow biopsy also demonstrated hemophagocytic lymphohistiocytosis, another disorder associated with elevated interferon-γ. Thus, his kidney disease was considered to represent a paraneoplastic process. Treatment of his NK cell leukemia led to correction of his serum creatinine value; however, proteinuria persisted.

Case 3 pathologic findings alone support a diagnosis of the collapsing variant of FSGS. The additional histologic changes of tubular injury, tubular microcystic change, and interstitial inflammation, and the clinical history of African American descent, should raise consideration for the diagnosis of *APOL1*-associated collapsing glomerulopathy. Investigation for potential factors that can cause collapsing glomerulopathy is essential to direct therapy toward targetable causes, such as HIV infection and treatment with antiretrovirals. In this instance, the

investigation led to the discovery of a rare neoplasm, NK cell leukemia, which was treated and resulted in the resolution of the patient's renal insufficiency, even though the proteinuria persisted. This case exemplifies how *APOL1*-associated nephopathies, and in particular *APOL1*-associated collapsing glomerulopathy, fit a two-hit model. The first hit is genetic; to date, there is no way to modify this. The second hit can be multiple, but interferons through infection, iatrogenic, or neoplastic sources constitute one of the hits that can cause this disease.

References

1. D'Agati VD, Fogo AB, Bruijn JA, Jennette JC. Pathologic classification of focal segmental glomerulosclerosis: a working proposal. *Am J Kidney Dis*. 2004;43(2):368–382.
2. Rao TK, Filippone EJ, Nicastri AD, et al. Associated focal and segmental glomerulosclerosis in the acquired immunodeficiency syndrome. *N Engl J Med*. 1984;310(11):669–673.
3. Wyatt CM, Klotman PE, D'Agati VD. HIV-associated nephropathy: clinical presentation, pathology, and epidemiology in the era of antiretroviral therapy. *Semin Nephrol*. 2008;28(6):513–522.
4. Markowitz GS, Nasr SH, Stokes MB, D'Agati VD. Treatment with IFN-alpha, -beta, or -gamma is associated with collapsing focal segmental glomerulosclerosis. *Clin J Am Soc Nephrol*. 2010;5(4):607–615.
5. Besse W, Mansour S, Jatwani K, Nast CC, Brewster UC. Collapsing glomerulopathy in a young woman with APOL1 risk alleles following acute parvovirus B19 infection: a case report investigation. *BMC Nephrol*. 2016;17(1):125.
6. Freedman BI, Limou S, Ma L, Kopp JB. APOL1-associated nephropathy: a key contributor to racial disparities in CKD. *Am J Kidney Dis*. 2018;72(5S1):S8–S16.
7. Kopp JB, Rosenberg AZ. One actor, many roles: histopathologies associated with APOL1 Genetic Variants. *Adv Anat Pathol*. 2019;26(3):215–219.
8. Nichols B, Jog P, Lee JH, et al. Innate immunity pathways regulate the nephropathy gene Apolipoprotein L1. *Kidney Int*. 2015;87(2):332–342.

Case 4 from Aasma Nalwa, MD-- All India Institute of Medical Sciences, Jodhpur, India

A 72-year-old white man with a history of coronary artery disease, hypertension, and type 2 diabetes mellitus presented with chills, fatigue, weakness, and fevers of unknown origin of several months' duration. His fevers spiked up to 104°F. He had severe balance issues, bi-temporal headaches, a nonproductive cough but no hemoptysis, and erratic blood sugars. There was no reported weight loss.

He denied any rash, but he had gone camping a month prior to the onset of the fevers, and he had a tick removed right after the trip. At that time, he was treated prophylactically with doxycycline. Other notable medications included trimethoprim and sulfamethoxazole (Bactrim) for 1 week for prostatitis, piperacillin and tazobactam (Zosyn) for presumed urinary tract infection, and hydralazine for hypertension.

On examination, the patient had a temperature of 99°F, BP 126/74 mm Hg, and pulse 85/min. There was no skin rash, lymphadenopathy, or hepatosplenomegaly; distal pulses were intact, and there was no peripheral edema. Urinalysis showed microscopic hematuria with few dysmorphic red blood cells (RBCs) and a urine protein-to-creatinine ratio of 0.5 mg/mg. Other laboratory test results included the following:

Hemoglobin	9.0 g/dL
White blood cell count	2400/µL
Platelets	8500/µL
Creatinine	2.5 mg/dL

Serologies at the time of hospital admission included the following:

- Positive anti-proteinase 3 (PR3) ANCA and negative anti-myeloperoxidase (MPO) ANCA
- Positive antinuclear antibody 1:102
- Negative anti-DNA antibody
- Low serum complement factor C3 (42) with normal complement factor C4 (21)
- Negative anti-GBM antibody

The patient was admitted to the hospital. Several days later, a renal biopsy was performed, at which time the serum creatinine concentration had increased to 3.8 mg/dL.

Light Microscopy:
The tissue for light microscopy contained 47 glomeruli: 1 with global sclerosis and 3 with early segmental tuft sclerosis with focal adhesions to Bowman's capsule. Segmental small cellular crescents were seen in two glomeruli, and one revealed a fibrous crescent. Focal fibrinoid tuft necrosis was seen in one glomerulus. There was diffuse acute tubular injury with scattered RBC casts. Blood vessels demonstrated mild to moderate intimal fibroelastosis. No vasculitis was seen.

Immunofluorescence Microscopy:
Sixteen glomeruli were available for the evaluation, of which none were sclerosed. There was granular glomerular mesangial and segmental capillary wall staining with antisera specific for IgA (3+), IgM (1+), C3 (4+), C1q (1+), and κ and λ light chains

(1+). No diagnostic staining was seen with antisera specific for IgG and fibrin. No extraglomerular staining was noted.

Electron Microscopy:
The semithin section demonstrated one glomerulus with mild mesangial expansion. Ultrastructural examination demonstrated GBMs of variable thickness with segmental basement membrane remodeling and segmental effacement of foot processes. Scattered mesangial, paramesangial, and subendothelial immune complex–type electron dense deposits were identified with no substructure.

Clinical Follow-up:
After the renal biopsy findings, the patient was advised to go back to the hospital for another workup for an infective endocarditis. On repeat transthoracic echocardiogram (TTE), small vegetations were noted on the prosthetic aortic valve. Unfortunately, he suffered a hemorrhagic stroke 3 days after the second hospital admission (thought to be due to septic emboli). The patient died and underwent a limited autopsy of the heart.

Gross examination of the aortic bioprosthetic valve showed multiple large vegetations. Histology sections from the valvular vegetations demonstrated areas with frank tissue necrosis and other areas with multinucleated giant cells and granulomatous inflammation. A Warthin-Starry stain and immunohistochemistry for *Bartonella* were both positive and showed numerous colonies of slender bacilli.

Questions for Case 4:

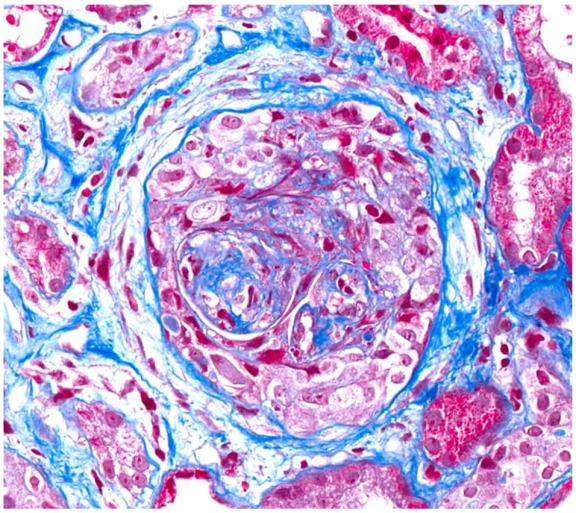

Figure 1

1. The morphological findings observed in Figure 1 can be due to which of the following?
   A. PR3 ANCA–associated necrotizing and crescentic GN
   B. Infection-associated GN
   C. Hydralazine-induced GN
   D. Membranoproliferative GN
   E. All the above

   Crescent formation is a general marker of disease activity; crescents do not uncover underlying disease etiologies. Thus, all of the listed disease entities can be associated with crescent formation, including drug-induced (e.g., hydralazine) glomerular inflammation.

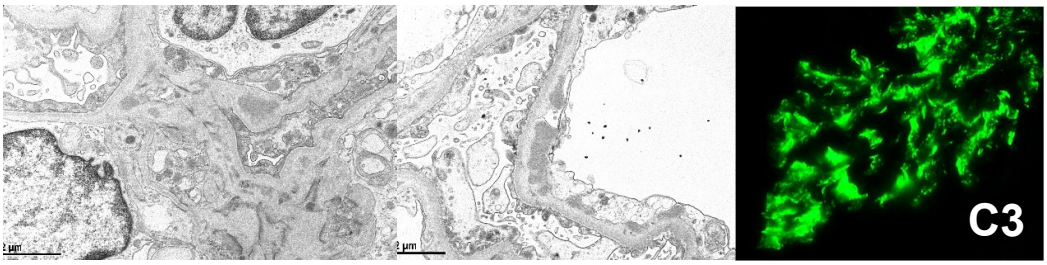

Figure 2

2. In the current case, immunofluorescence staining showed granular mesangial and segmental capillary wall staining for IgG (0), IgA (3+), IgM (1+), C3 (4+), C1q (1+), and κ and λ light chains (1+).

   Is the detection of subendothelial and mesangial immune complex deposits by electron microscopy along with dominant C3 staining by immunofluorescence (Figure 2) diagnostic for a C3 GN?
   A. Yes
   B. No

The key diagnostic feature of a C3 GN is sole or dominant C3 staining by immunofluorescence (with more intense C3 staining, i.e., two grades more than seen for any other immunoglobulin). This definition is not met in the current case. In addition, note fibrinoid glomerular tuft necrosis is usually not detected in C3 glomerulonephritides.

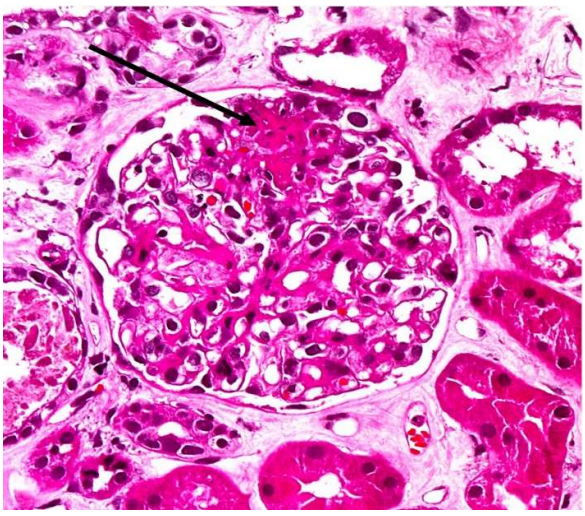

Figure 3

3. Segmental fibrinoid tuft necrosis in glomeruli lacking significant proliferative changes (Figure 3) can be seen in which of the following?
   A. PR3 ANCA–associated GN
   B. Infective endocarditis
   C. MPO ANCA–associated GN
   D. Anti-GBM disease
   E. Segmental lupus nephritis
   F. All of the above

Although fibrinoid glomerular tuft necrosis is typically found in anti-GBM or ANCA-induced glomerulonephritides, the same pattern of injury can also be seen with other underlying etiologies. Diagnostically most challenging are necrotizing glomerulonephritides caused by infectious endocarditis that can show overlap with ANCA disease.

Differential Diagnosis:

1. Infection-associated GN
2. PR3 ANCA–associated necrotizing and crescentic GN
3. Hydralazine-associated lupus-like GN

The constellations of findings are of a necrotizing and crescentic GN that is not a specific disease but an indicator of severe glomerular injury causing rapidly progressive renal failure. It is important to identify the underlying cause of crescentic GN to provide optimum treatment. Based on the morphologic features by light microscopy, and the pattern of immune deposition by immunofluorescence and electron microscopy, these lesions can be classified into three major etiologic categories: pauci-immune GN, anti-GBM antibody GN, and immune complex–mediated GN. The absence of anti-GBM antibody in the serum and lack of linear deposits for IgG on immunofluorescence ruled out an anti-GBM antibody–mediated etiology. The presence of PR3 ANCA suggested a pauci-immune etiology. However, other unusual findings, such as low serum complement level factor C3, presence of strong C3 and IgA staining by immunofluorescence, and subendothelial and mesangial deposits on electron microscopy, were more suggestive of an immune complex–mediated underlying etiology. The most likely possibilities were a drug-induced lupus GN from hydralazine or an infection-associated GN due to an underlying occult infection such as endocarditis. Lupus GN typically demonstrates IgG-dominant staining by immunofluorescence along with more intense C1q staining as opposed to the current case, which shows C3- and IgA-dominant deposits.

On further discussion of the biopsy findings with the clinician, it was noted that the patient had a bioprosthetic aortic valve replacement 2 years back. He also revealed exposure to barn cats; he had been scratched multiple times by the cats. His blood cultures so far were negative, and a TTE was negative for any aortic valve vegetations. An infectious disease workup revealed that serology for *Bartonella henselae* IgG antibody was positive at 1:1024.

Diagnosis

Bartonella infection-associated focal necrotizing and sclerosing GN with 4% cellular crescent formation.

Discussion

Cat scratch disease caused by *Bartonella henselae* comes primarily from the bite or scratch of cats harboring the bacterium. It is relatively benign and self-limiting, lasting 6-12 weeks in the absence of antibiotic therapy, and is characterized by a mild infection at the point of injury, fever, and regional lymphadenopathy. Various systemic complications include osteomyelitis, encephalitis, splenomegaly, and necrotizing hepatic lesions. Of all cases of infective endocarditis, the incidence of blood culture–negative endocarditis by *Bartonella* species varies from 5% to 30%.[1] The majority of *Bartonella henselae* endocarditis cases have a history of exposure to cats and a preexisting prosthetic valve, similar to our patient. Glomerulonephritis can

be a complication of *Bartonella henselae*-induced endocarditis. It has been observed that the most common presentation in such cases is acute renal failure rather than nephritic syndrome.[2] On immunofluorescence examination of renal biopsies, C3 staining was present in all cases, and staining with IgA was present in 28% of cases, along with electron microscopy demonstrating immune complex deposits in mesangial and subendothelial locations.[2] Our case had dominant C3 (3+) and IgA (3+) staining with detectable immune complexes in the mesangial and subendothelial regions on electron microscopy. The presence of IgA (3+) staining contradicts a diagnosis of C3 GN, in which the intensity of C3 staining should be at least two grades higher than any other immunoglobulin and show no staining for C1q (the current case demonstrated 1+ staining for C1q).[3]

Another notable finding in the current case was the presence of a positive PR3 ANCA titer. The presence of ANCA in the setting of a necrotizing and crescentic GN due to *Bartonella henselae* infective endocarditis has been previously reported in a number of case reports.[5-9]

What is the association between PR3 ANCA antibodies and infective endocarditis? Are there antibodies against complementary peptides of PR3 (i.e., that are directed against a PR3 antisense peptide) coded by the *Bartonella* genome? Microbes are known to carry complimentary proteins that are molecular mimics of known autoantigens. [10]

Disease	Species
Sjogren's syndrome	*Baizongi pistaciae*, *Streptomyces avermitilis*, *Magnetospirillum magnetotacticum*, *Leptospira interrogans*, *Plasmodium falciparum*, *Neurospora crassa*, *Helicobacter pylori*, *Bacillus anthracis*, *Streptococcus pneumoniae*, *Caulobacter crescentus*
Bullous pemphigoid	*Listeria monocytogenes*, *Listeria innocua*, *Pyrococci abyssi*, *Rhodopirellula baltica*, *Nodularia spumigena*, *Nostoc punctiforme*, *Anopheles gambiae*, *Neurospora crassa*, *Clostridium acetobutylicum*, *Clostridium tetani*
Autoimmune thyroiditis	*Dictyostelium discoideum*, *Rhodospirillum rubrum*, *Streptomyces coelicolor*, *Escherichia coli*, *Pseudomonas putida*, *Chlorobium tepidum*, *Candida glabrata*, *Thermotoga maritima*, *Lactococcus lactis*, *Azotobacter vinelandii*
Myasthenia gravis	*Corynebacterium diphtheriae*, *Sulsolbus tokodaii*, *Giardia lamblia*, *Sinorhizobium meliloti*, *Clostridium tetani*, *Chlamydiae Parachlamydia* spp., *Gyrodactylus salaris*, *Gyrodactylus thymalli*, *Gordionus violaceus*, *Trichodesmium erythraeum*
Anti-GBM disease (Goodpasture's disease)	*Pseudomonas fluorescens*, *Shewanella oneidensis*, *Bacillus halodurans*, *Blepharisma japonicum*, *Burkholderia fungorum*, *Cyanobacterium Synechococcus* spp., *Ustilago maydis*, *Nostoc punctiforme*, *Cymopterus watsonii*

Microbes introduce complementary PR3 peptides (cPR3), inducing an immune response that leads to the production of anti-cPR3 antibodies. These anti-cPR3 antibodies then act as an “antigen,” leading to the development of anti-idiotypic antibodies that recognize not only the complementary cPR3 but also the portion of the PR3 molecule to which the peptide is complementary.[10]

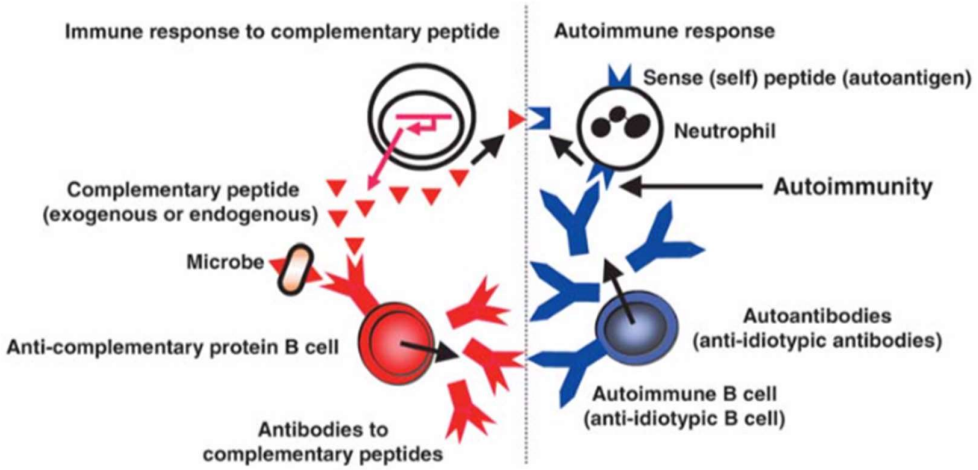

Figure courtesy of Pendergraft et al.[12]

Many microbes have been recognized that carry proteins complementary to known autoantigens.[12]

Take-Home Points

- *Bartonella henselae* endocarditis may present with a necrotizing and crescentic GN and elevated PR3 ANCA antibodies, thus mimicking an ANCA-associated vasculitis.
- Necrotizing and crescentic GN can be the initial presentation of a *Bartonella*-associated endocarditis.
- Because *Bartonella* is fastidious and often does not grow in blood cultures (culture-negative endocarditis), clinical symptoms and lab results may lead to an incorrect diagnosis of ANCA vasculitis.
- An incorrect diagnosis may expose patients to immunosuppressive regimens that are potentially hazardous to patients with infectious endocarditis.
- If an initial TTE study is negative, and clinical suspicion for endocarditis remains elevated, follow your instincts and repeat the study within 4–5 days.
- Clinical suspicion should never be abandoned even in the face of “confirmatory” lab tests.
- In this case, another TTE was eventually done when the renal biopsy results did not correlate with the clinical diagnosis of ANCA vasculitis, but it was unfortunately too late.

References

1. Tattevin P, Watt G, Revest M, Arvieux C, Fournier P-E. Update on blood culture-negative endocarditis. *Med Mal Infect*. 2015;45(1–2):1–8.

2. Boils CL, Nasr SH, Walker PD, Couser WG, Larsen CP. Update on endocarditis-associated glomerulonephritis. *Kidney Int*. 2015;87(6):1241–1249.

3. Sethi S, Fervenza FC, Zhang Y, et al. C3 glomerulonephritis: clinicopathological findings, complement abnormalities, glomerular proteomic profile, treatment, and follow-up. *Kidney Int*. 2012;82(4):465–473.

4. Nasr SH, Radhakrishnan J, D'Agati VD. Bacterial infection–related glomerulonephritis in adults. *Kidney Int*. 2013;83(5):792–803.

5. Vikram HR, Bacani AK, DeValeria PA, Cunningham SA, Cockerill FR. Bivalvular Bartonella henselae prosthetic valve endocarditis. *J Clin Microbiol*. 2007;45(12):4081–4084.

6. Khalighi MA, Nguyen S, Wiedeman JA, Palma Diaz MF. Bartonella endocarditis–associated glomerulonephritis: a case report and review of the literature. *Am J Kidney Dis*. 2014;63(6):1060–1065.

7. Turner J, Pien B, Ardoin S, et al. A man with chest pain and glomerulonephritis. *Lancet*. 2005;365(9476):2062.

8. Salvado C, Mekinian A, Rouvier P, Poignard P, Pham I, Fain O. Rapidly progressive crescentic glomerulonephritis and aneurism with antineutrophil cytoplasmic antibody: Bartonella henselae endocarditis. *Presse Med*. 2013;42(6):1060–1061.

9. Vercellone J, Cohen L, Mansuri S, Zhang PL, Kellerman PS. Bartonella endocarditis mimicking crescentic glomerulonephritis with PR3-ANCA positivity. *Case Rep Nephrol*. 2018;2018:9607582.

10. Preston GA, Pendergraft WF 3rd, Falk RJ. New insights that link microbes with the generation of antineutrophil cytoplasmic autoantibodies: the theory of autoantigen complementarity. *Curr Opin Nephrol Hypertens*. 2005;14(3):217–222.

11. Pendergraft WF 3rd, Pressler BM, Jennette JC, Falk RJ, Preston GA. Autoantigen complementarity: a new theory implicating complementary proteins as initiators of autoimmune disease. *J Mol Med (Berl)*. 2005;83(1):12–25.

Case 5 from Parmjeet S. Randhawa, MD MBBS from University of Pittsburgh

A 50-year-old white woman with morbid obesity, a BMI of 42, hypertension, sleep apnea, diabetes mellitus, and recurrent hypoglycemic episodes underwent a Roux-en-Y gastric bypass procedure. A liver biopsy performed during the surgery showed non-alcoholic steatohepatitis, with 50% macrovesicular steatosis, a hepatic activity index of 4 (on a scale of 0–8), and a fibrosis stage of 2 (on a scale of 0–4).

The surgery helped the patient reduce her BMI to 28 but led to progressive renal failure. A native kidney biopsy was performed and was described as having acute tubular injury superimposed on moderate to severe arteriosclerosis and mild to moderate arteriolar hyalinosis. It was noted that the glomeruli did not show changes of diabetic nephropathy. Moreover, her blood glucose levels were well controlled, and her hemoglobin A_{1c} level was 4.1%. One month after the native kidney biopsy, she presented to the emergency department with an episode of sudden, severe abdominal pain, which resolved spontaneously. It was postulated that she had passed a kidney stone, and she was discharged to continue hemodialysis.

A living non-related donor transplant was performed 7 years after the bypass surgery and 1 year after initiation of hemodialysis. The immunosuppression regimen consisted of thymoglobulin induction and maintenance therapy with tacrolimus 6 mg twice daily and mycophenolate mofetil 500 mg twice daily. The patient achieved a serum creatinine nadir of 0.8 mg/dL and had her ureteric stent removed successfully 6 weeks after surgery. Two months after transplantation, her serum creatinine increased to 1.2 mg/dL after a reduction in the dose of mycophenolate mofetil because of gastrointestinal adverse effects. The biopsy showed Banff 1A T-cell–mediated rejection with no C4d staining. Mild interstitial fibrosis/tubular atrophy (IFTA) was observed and considered to represent donor disease. Test results for cytomegalovirus, polyomavirus, BK virus, and donor-specific antibodies were negative. The patient responded well to three doses of solumedrol and was clinically stable.

Laboratory investigations at 3 months post-transplant yielded the following values:

Hemoglobin	10.1 g/dL
Hematocrit	30.4%
White blood cell count	9900/μL
Serum bilirubin	0.5 mg/dL
Aspartate aminotransferase	12 U/L
Alanine aminotransferase	14 U/L
Serum alkaline phosphatase	75 U/L
Serum γ-glutamyltransferase	18 U/L
Serum calcium	9.1 mg/dL

The urine was clear with negative test results for blood, bilirubin, nitrates, glucose, and ketones. The urine sediment examination revealed 1 red blood cell and 4 white blood cells per high-power field. Urine protein content was 17 mg/dL. Testing performed earlier at the time of transplantation was negative for hepatitis B surface antigen, hepatitis C virus serology, antinuclear antibodies, and rheumatoid factor. Serum complement levels C3 and C4 were in the normal range. Immune electrophoresis and serum κ/λ levels did not demonstrate any paraproteins.

A protocol biopsy was performed 3 months after transplantation as a part of routine clinical care.

Questions for Case 5:

1. Refer to the representative figure from an allograft biopsy performed 2 weeks post-transplant for increasing serum creatinine (periodic acid–Schiff [PAS] stain). This transplant was performed for primary FSGS. Which of the following is the best description of the pathology that is illustrated?
   A. Peritubular capillaritis representing an early stage of antibody-mediated rejection
   B. Interstitial inflammation heralding acute T-cell–mediated rejection
   C. Acute tubular injury due to dehydration
   D. Proteinuria due to recurrent disease
   E. Obstruction due to a stone in the ureter

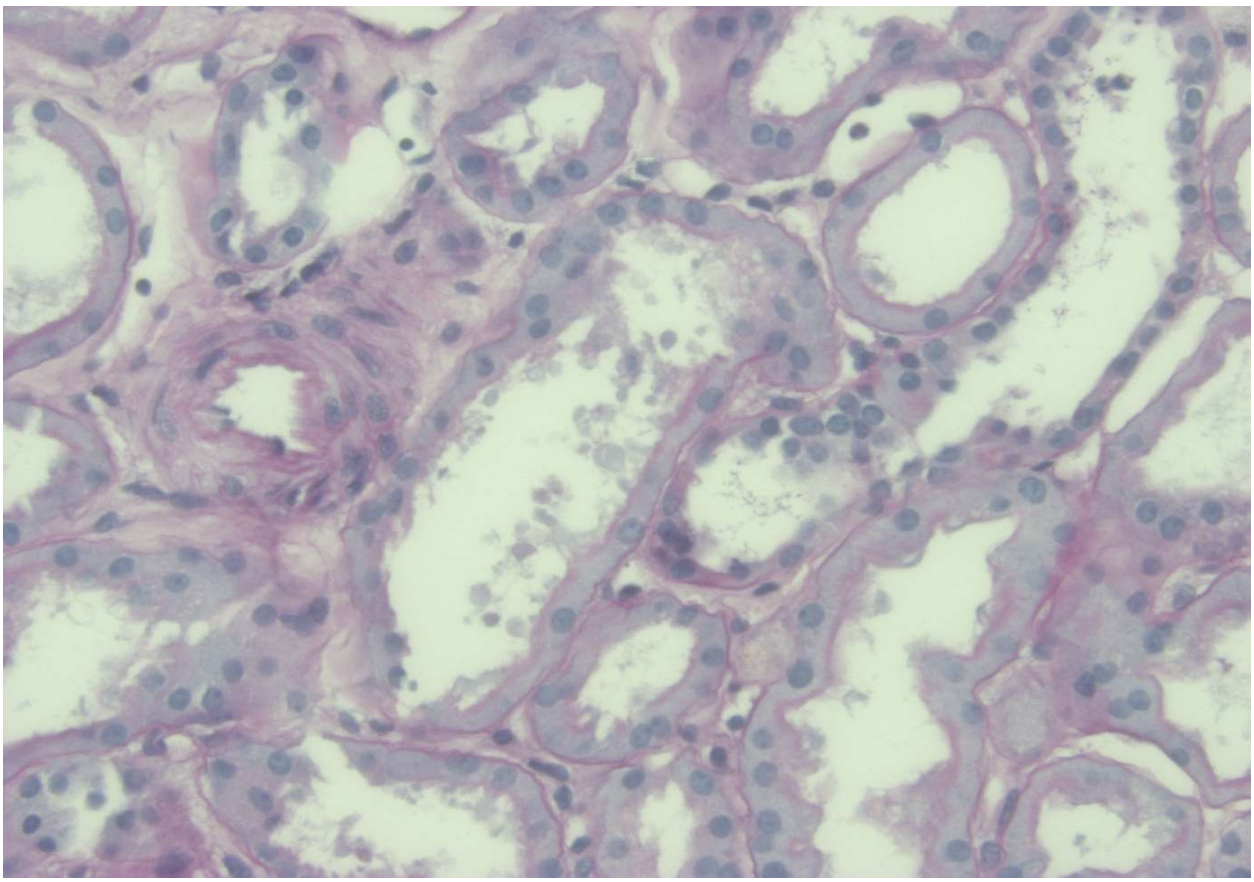

Acute tubular injury. The tubules are dilated and contain granular proteinaceous material. The brush border is seen as a pink band toward the luminal aspect of the tubular epithelium. Although it forms a continuous line in some tubules, in others it is focally lost, reflecting ischemic injury to the microvilli. A few lymphocytes are present in the peritubular capillaries but do not exceed the threshold of 3–4 cells per capillary required for a diagnosis of peritubular capillaritis. The minimal interstitial inflammation is quite compatible with a reaction to tubular injury and is insufficient to entertain a diagnosis of T-cell–mediated rejection. Proteinuria would be characterized by cast formation. Obstruction due to stones can cause tubular dilatation but would be extremely unlikely in a biopsy performed 2 weeks post-transplant.

2. The next figure is from a kidney allograft biopsy examined under polarization microscopy. What inference can be made about the patient from the brightly shining structures?
   A. Oxaluria
   B. Proteinuria
   C. Lipiduria
   D. Hematuria
   E. Bilirubinuria

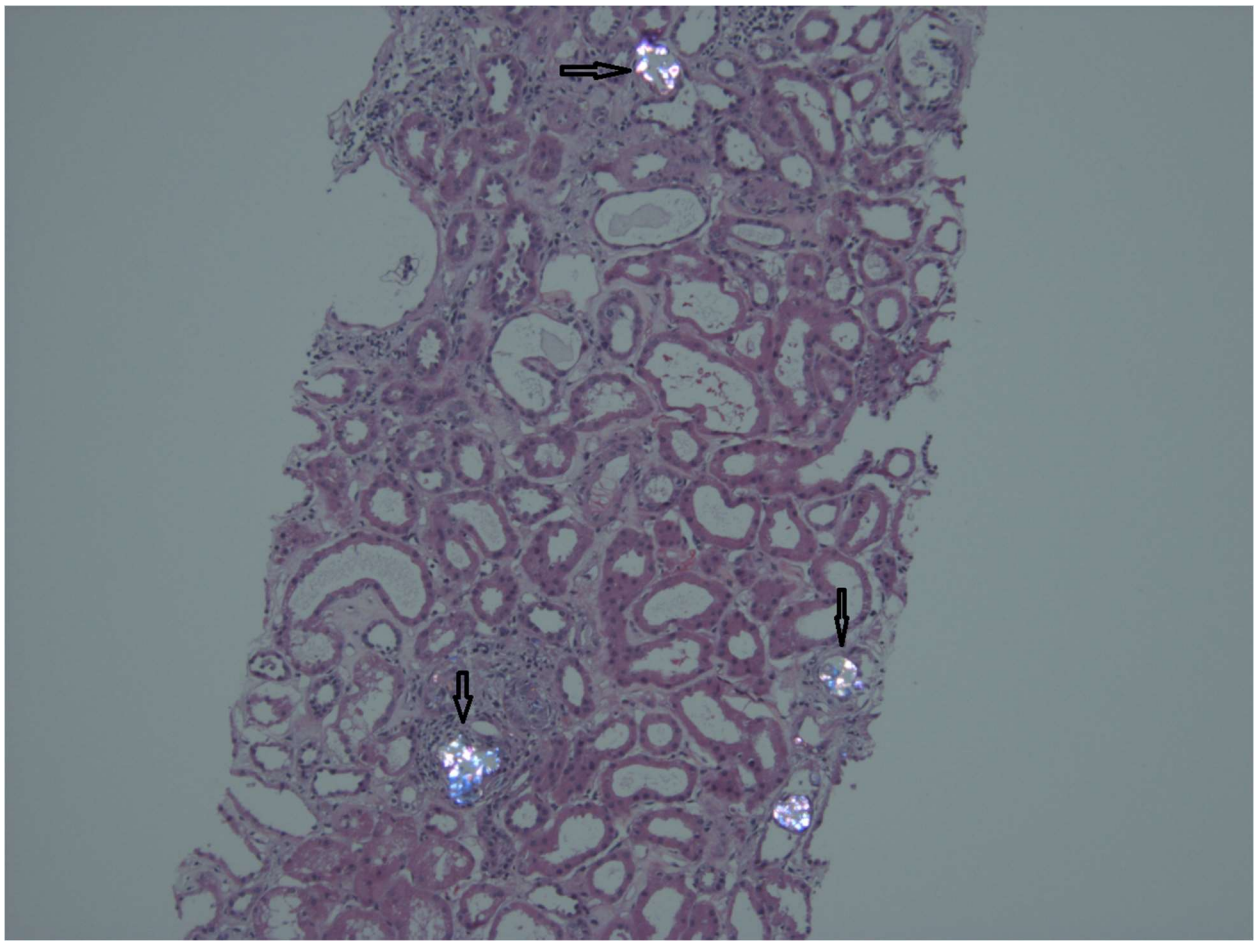

Oxalate crystals are characteristically birefringent on polarization microscopy. Proteinuria is associated with tubular casts that do not polarize. Lipiduria may be accompanied by colorless cholesterol crystals, which can polarize but with a Maltese-cross pattern that is not seen here. Hematuria is recognized by red blood cells or red cell casts and bilirubinuria by casts that have a greenish hue. Neither red cells nor bilirubin shows birefringence on polarization.

3. The bluish globular structures seen in this kidney biopsy figure (hematoxylin and eosin [H&E] stain) represent which of the following?
   A. Calcium oxalate
   B. Calcium phosphate
   C. Cholesterol
   D. 2,8-Dihydroxyadenine
   E. Hemoglobin

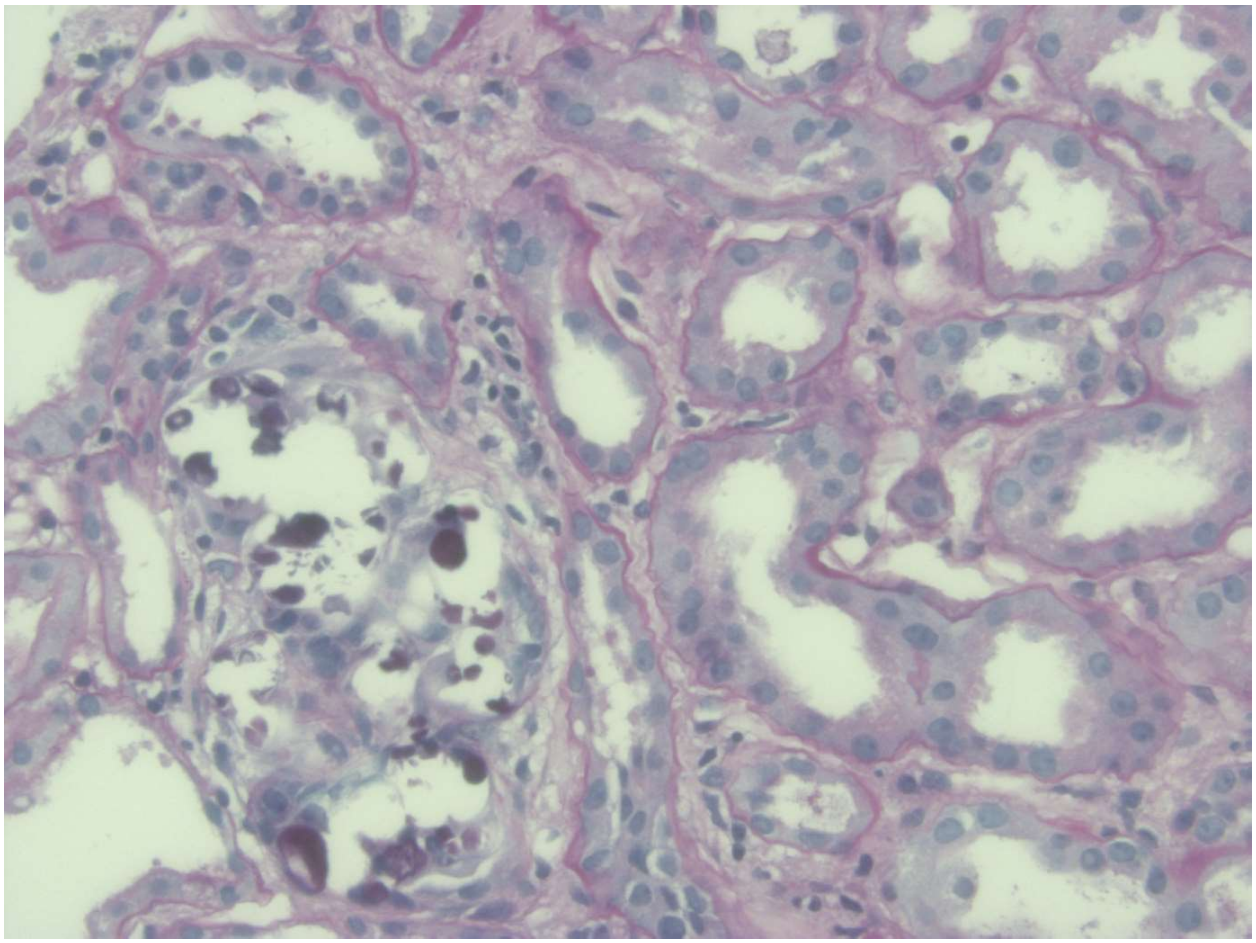

Calcium phosphate is recognized by spherical to oval deposits of an acellular material that appears blue with H&E stain. Although not usually necessary, a confirmatory von Kossa stain can be performed, and it would impart a black color to these deposits. Oxalate crystals polarize. Cholesterol crystals are colorless, as mentioned in question 2. Crystals of 2,8-dihydroxyadenine are reddish brown in color, and some can polarize with a Maltese cross appearance. Hemoglobin has a reddish hue, typically accompanied by red blood cells and red cell casts. Immunohistochemical confirmation is desirable because myoglobin can have an identical appearance.

Diagnosis

1. Recurrent oxalosis secondary to enteric hyperoxaluria.
2. Crystalline nephropathy with acute interstitial nephritis and tubulitis.
3. Mild arteriosclerosis, arteriolar hyalinosis, interstitial fibrosis, and tubular atrophy.

Discussion:

The tubules are dilated with focal areas of flattened lining epithelium. The PAS stain shows discontinuities in the brush border that normally lines the luminal surface of the tubular epithelium in a continuous fashion. Many tubules contain cell debris, shed epithelial cells, and proteinaceous casts. Others show regenerative activity in the form of enlarged nuclei, prominent nucleoli, cytoplasmic basophilia, and mitotic activity. An important finding is the presence of interstitial and intratubular crystalline material that shows brilliant birefringence on polarization microscopy. This appearance is characteristic of calcium oxalate crystals. A 24-hour urine collection had an oxalate concentration of 151 mg/g creatinine (reference range 1.6–37.0 mg/g).

The biopsy also contains a mild interstitial inflammatory infiltrate that consists predominantly of mononuclear cells. At places, this infiltrate traverses the tubular basement membranes and produces the lesion referred to as tubulitis. The tubules show mild atrophy, as judged by their decreased diameter and thickened basement membranes. The latter finding is best appreciated with a PAS stain. The biopsies also show a mild increase in collagen fibers in the stroma (interstitial fibrosis). The intimal layer of the arteries is normally imperceptible, but in this biopsy, it is expanded because of arteriosclerosis. The arteriolar walls contain PAS-positive fluid material that is referred to as arteriolar hyalinosis. Most glomeruli have patent capillary loops with no evidence of intracapillary inflammation (glomerulitis) or duplication of GBMs (chronic transplant glomerulopathy). However, 2 of 20 glomeruli are globally sclerotic and consist entirely of scar tissue, which has obliterated all the capillary loops and is filling up the urinary space. The mild histologic chronicity in this biopsy can be attributed to a combination of donor disease and ongoing interstitial inflammation.

Differential Diagnosis:

The commonest cause of interstitial inflammation and tubulitis in early post-transplant biopsies is acute T-cell–mediated rejection. Indeed, this was the original interpretation of this biopsy and led to steroid pulse therapy. However, subsequent review at a quality assurance conference led to the observation that the severity of the tubular injury was out of proportion to the degree of inflammation. In addition, intratubular oxalate crystals were noted, and a diagnosis of crystalline nephropathy was rendered.

Tubulitis in biopsies is an important feature for the diagnosis of T-cell–mediated rejection but is not absolutely specific for this diagnosis. The interstitial inflammation in bacterial or viral infection, drug hypersensitivity reactions, GN, paraproteinemia, and post-transplant lymphoproliferative disease can also infiltrate the tubular epithelium. This results in lesions that can mimic tubulitis. The correct diagnosis can be made from the clinical context and associated pathology findings. For example, pyelonephritis will be characterized by intratubular neutrophil clusters and white cell casts. Viral cytopathic effect and immunohistochemistry for viral antigens can establish the diagnosis of polyomavirus nephropathy. Glomerulonephritis will frequently have immune complex deposits. Paraproteins are recognized by demonstrating immunoglobulin light chain restriction on immunofluorescence. Post-transplant lymphoproliferative disease will

typically be a B-cell rather than T-cell infiltrate and will also test positive for Epstein-Barr virus–encoded EBER RNA (although Epstein-Barr virus–negative lesions can also be sometime encountered). Molecular tests for T-cell–mediated rejection, such as the so-called molecular microscope based on Affymetrix microarray technology, have been touted as specific for alloimmune injury. However, sufficient numbers of the conditions that can mimic rejection have not been tested using this modality. It is likely that common mechanisms of T-cell infiltration and resulting tissue injury will result in substantial overlap in the molecular signatures of these diseases.

Oxalate crystals in this biopsy were recognized by the morphologic appearance, polarization microscopy, and elevated serum and urine oxalate levels. Histopathologic examination can also identify several other clinically relevant crystalline nephropathies. For example, calcium phosphate crystals occur in conditions of elevated serum calcium (e.g., secondary or tertiary hyperparathyroidism) and prior acute tubular injury (so-called dystrophic calcification). These are non-refractile and acquire a blue color on von Kossa stain. Less commonly encountered causes of crystalline nephropathy include gout, a variety of medications (particularly sulfonamides, antiretroviral drugs, triamterene, and methotrexate), immunoglobulin light chain crystals in paraproteinemia, and 2,8-dihydroxyadenine crystals in adenine phosphotransferase deficiency.

Morbid obesity is commonly treated by gastric bypass operations. These surgical interventions can result in malabsorption and steatorrhea secondary to a short gut syndrome. Binding of free calcium to excessive free fatty acids in the bowel lumen reduces the precipitation of dietary oxalate into insoluble calcium oxalate. Overabsorption of free oxalate through the colonic mucosa can result in systemic oxalosis, one manifestation of which can be chronic renal failure. This problem is particularly likely to happen after a jejuno-ileal bypass, which can result in food bypassing long segments of the small intestine. For this reason, this procedure has been abandoned in favor of procedures such as Roux-en-Y gastric bypass, gastroplasty, and gastric banding.

This case draws attention to the problem of oxalate nephropathy that can develop after bypass surgery to treat severe obesity. If oxalate overabsorption is not kept in mind at the time of transplantation, and not appropriately managed by post-transplant care providers, the disease can tragically recur in the allograft. Initially, this patient was managed conservatively with a low-fat and low-oxalate diet, high fluid intake, oral calcium with meals, and potassium citrate, but graft dysfunction progressed, and dialysis had to be initiated. At this point, it was decided to reverse the gastric bypass by a second surgical intervention. Graft function started improving, and it was possible to wean the patient off dialysis 6 weeks after surgery. The patient's most recent serum creatinine was 2.3 mg/dL. A repeat biopsy showed a reduction in oxalate crystals and improvement in associated tubular injury. Her urine oxalate level decreased from a peak of 151 mg/24 hours to 37 mg/24 hours (normal range 3.6-38 mg/24 hours). Correspondingly, the plasma oxalate decreased from 64 μmol/L to within the normal range (< 2.5 μmol/L). Further monitoring of the patient will focus on the development of nephrocalcinosis and nephrolithiasis and recurrent episodes of obstruction and urosepsis.

In summary, controlling significant enteric hyperoxaluria in a renal allograft is a challenging medical problem. It should be kept in mind that reversal of the gastric bypass is a viable option to effectively manage this and other severe complications that can result from bariatric surgery.

References:

1. Nazzal L, Puri S, Goldfarb DS. Enteric hyperoxaluria: an important cause of end-stage kidney disease. *Nephrol Dial Transplant*. 2016;31(3):375–382.

2. Daudon M, Frochot V, Bazin D, Jungers P. Drug-induced kidney stones and crystalline nephropathy: pathophysiology, prevention, and treatment. *Drugs*. 2018;78(2):163–201.

3. Gwinner W, Suppa S, Mengel M, et al. Early calcification of renal allografts detected by protocol biopsies: causes and clinical implications. *Am J Transplant*. 2005:5:1934–1941.

4. Upala S, Jaruvongvanich V, Sanguankeo A. Risk of nephrolithiasis, hyperoxaluria, and calcium oxalate supersaturation increased after Roux-en-Y gastric bypass surgery: a systematic review and meta-analysis. *Surg Obes Relat Dis*. 2016;12(8):1513–1521.

5. Ekser B, Mangus RS, Kubal CA, et al. Recurrence of hyperoxaluria and kidney disease after combined intestine-kidney transplantation for enteric hyperoxaluria. *Am J Nephrol*. 2016;44(2):85–91.

6. Moon RC, Frommelt A, Teixeira AF, Jawad MA. Indications and outcomes of reversal of Roux-en-Y gastric bypass. *Surg Obes Relat Dis*. 2015;11(4):821–826.